Atomic decay in a coupled-cavity system with Gaussian-correlated hopping

R. A. Silva[a], H. R. Publio[a], A. J. F. de Souza[a], G. M. A. Almeida[b,*], A. L .R. Barbosa[a], F. A. B. F. de Moura[a,b,**]

[a]*Departamento de Física, Universidade Federal Rural de Pernambuco, 52171-900 Recife, PE, Brazil*
[b]*Instituto de Física, Universidade Federal de Alagoas, 57072-900 Maceió, AL, Brazil*

Abstract

We investigate the dynamics of a two-level atom weakly interacting with a one-dimensional chain of coupled cavities with spatially-correlated hopping disorder. The correlations are introduced via a Gaussian kernel and enable the emergence of quasi-extended modes despite the presence of fluctuations. By tracking the time evolution of the excitation, we observe a crossover between Markovian to non-Markovian decay regimes. For larger correlation lengths, the Markovian dynamics is pronounced when the atomic frequency meets a well defined region around the center of the photonic band, indicating the presence of the delocalized modes. Our results highlight the role of correlated structural disorder in controlling the dynamics of open quantum systems as well as probing transport properties of low-dimensional systems.

1. Introduction

In the process of spontaneous emission of a two-level atom, the dynamics the emitted energy depends on the geometry of the surroundings [1, 2]. In open space, the excitation decays exponentially and never returns to the atom, due to the flat profile of the associated spectral density. In contrast, when the spectral density is characterized by a narrow spectral lineshape (e.g. a high-Q cavity) the atom can reabsorb and emit the photon multiple times, a phenomenon known as vacuum Rabi oscillations. In terms of information backflow and non-Markovianity [3], these two events lie at opposite ends, the former being classified as a Markovian (memoryless) amplitude damping process. Non-Markovian dynamics is therefore expected when the atom is coupled to structured environments possessing nontrivial spectral densities, a scenario explored in various contexts [2, 4, 5, 6, 7, 8, 9, 10, 11, 12, 13, 14, 15, 16, 17, 18, 19, 20, 21]. In this respect, photonic crystals offer a rich platform to study and manipulate light-matter interactions, and have indeed seen significant experimental progress [22, 23, 24, 25, 26, 27].

Structured (or colored) environments can be engineered from simple geometries such as 1D tight-binding models [28, 29, 11, 12, 14, 20, 21] and still allow for involved dynamics. In Ref. [11], Lorenzo *et al.* considered a single two-level emitter locally coupled to an array of cavities with evanescent field modes. In the presence of on-site Anderson disorder, they showed that the onset of localized single-photon modes led to a non-Markovian regime of atomic emission; in contrast to the Markovian behavior supported by the effectively flat spectral density around the center of the band. Monteiro *et al.* [20] extended this idea by considering a long-range correlated disorder model known to support a localization-delocalization transition [30]. The degree of non-Markovianity could be judiciously controlled by the correlation parameter. In another recent work [21], a coupled-cavity array featuring short-range correlated defects was considered, revealing a crossover from non-Markovian to Markovian regimes at specific resonances.

Inspired by the prospect of performing cavity QED in disordered lattices [22], some of the findings above highlight the role of anomalous transport in low-dimensional systems with correlated disorder [31], where standard Anderson localization breaks down. These models are promissing for designing photonic lattices to control the emission process. Conversely, the emitter dynamics can be used probe the transport properties of the environment, allowing for, e.g., spectral density learning and classification [32, 33].

In previous works [11, 12, 20, 21] the influence of on-site disorder in a coupled-cavity array, encoded in the cavity frenquencies, was considered. This time, we address the role of hopping (off-diagonal) disorder displaying Gaussian correlations [34], where spatial correlations decay smoothly with distance. The environment now enjoys chiral symmetry and, unlike the standard Anderson model with diagonal disorder, off-diagonal disorder can lead to critical behavior at zero energy [31]. All eigenstates remain localized in one dimension, but the wavefunctions display power-law decay, instead of exponential decay, near the band center. Our goal is to investigate how this affects the atomic emission process. We observe a crossover from non-Markovian to Markovian decay around the center of the band for larger correlation lengths, thereby confirming the presence of nearly delocalized environment modes.

2. Model

2.1. General

Let us consider a single two-level atom weakly coupled to the field mode supported by a high-Q cavity. The resulting Jaynes-

*Email: gmaalmeida@fis.ufal.br
**Email: fidelis@fis.ufal.br

Cummings interaction is written as ($\hbar = 1$)

$$\hat{H}_I = \omega_a \hat{\sigma}_+ \hat{\sigma}_- + \gamma(\hat{\sigma}_+ \hat{a}_0 + \hat{\sigma}_- \hat{a}_0^\dagger), \tag{1}$$

where $\hat{a}_0$, $\hat{a}_0^\dagger$ are the bosonic operators acting on the cavity mode, σ_+, σ_- are the atomic ladder operators, ω_a is the corresponding transition frequency between ground and excited states, $\{|g\rangle, |e\rangle\}$, and γ denotes the interaction strength. Such a model is paradigmatic in quantum optics and has been extensively used to describe light–matter interactions in cavity QED. If the atom is initialized in the excited state with the cavity in the vacuum, Rabi oscillations take place at a frequency given by γ.

Viewing the cavity mode as a quantum reservoir, we realize that the atomic decay problem (an amplitude damping channel) is rather trivial and distinguished by periodic memory revivals. This scenario can thus be regarded as fully non-Markovian [2, 11]. A natural extension is to consider the atom interacting with many bosonic modes $\hat{\alpha}_k$, with associated frequencies E_k, described by the so-called spin-boson Hamiltonian [35]

$$\hat{H} = \omega_a \hat{\sigma}_+ \hat{\sigma}_- + \sum_k E_k \hat{\alpha}_k^\dagger \hat{\alpha}_k + \sum_k \gamma_k (\hat{\sigma}_+ \hat{\alpha}_k + \hat{\sigma}_- \hat{\alpha}_k^\dagger). \tag{2}$$

Considering the joint atom-environment initial state $|\psi(0)\rangle = |e\rangle|\text{vac}\rangle$, its unitary time-evolution yields $|\psi(t)\rangle = e^{-iHt}|\psi(0)\rangle = f_e(t)|e\rangle|\text{vac}\rangle + \sum_k f_k(t)|g\rangle|\alpha_k\rangle$, where $|\alpha_k\rangle = \hat{\alpha}_k^\dagger|\text{vac}\rangle$ denotes a single-photon occupying field mode k and $f_e(t)$, $f_k(t)$ are time-dependent coefficients. Straightforward manipulations lead to the equation for $f_e(t)$ [11]:

$$\dot{f}_e(t) = -i\omega_a f_e(t) - \int_0^t \sum_k \gamma_k^2 e^{-iE_k(t-t')} f_e(t') dt', \tag{3}$$

where we identify the spectral density of the reservoir as $G(E) \equiv \sum_k |\gamma_k|^2 \delta(E - E_k)$, which fully characterizes it. In general, compared to Eq. (1), the atomic excitation spreads into the modes in a more complicated manner. The standard Markovian regime of emission, characterized by exponential decay, is obtained when $G(E)$ is constant (or at least varies smoothly over an appreciable range of frequencies). In this case the atom sees a flat, unstructured environment.

2.2. Disordered coupled-cavity array

We now provide a structure to the environment by assuming that the cavity described by Eq. (1) is part of an array of coupled (empty) $N + 1$ cavities featuring a 1D tight-binding description given by

$$\hat{H}_{\text{env}} = \sum_{i=-N/2}^{N/2} \epsilon_i \hat{a}_i^\dagger \hat{a}_i + \sum_{i=-N/2}^{N/2-1} J_i \left(\hat{a}_i^\dagger \hat{a}_{i+1} + \hat{a}_{i+1}^\dagger \hat{a}_i \right), \tag{4}$$

where J_i is the hopping strength expressed in units of $J \equiv 1$. The full Hamiltonian thus reads $\hat{H} = \hat{H}_I + \hat{H}_{\text{env}}$ and describes the two-level atom locally coupled to the array via the central cavity ($i = 0$). The connection to Eq. (2) is established from $\hat{H}_{\text{env}}|\alpha_k\rangle = E_k|\alpha_k\rangle$ and $\gamma_k = \gamma\langle\text{vac}|\hat{a}_0|\alpha_k\rangle$.

In this work, we assume that the cavity frequencies are assumed to be uniform and set to zero for simplicity $\epsilon_i \equiv 0$.

On the other hand, the cavity-cavity couplings J_i are generated from a Gaussian-correlated random sequence, defined as $J_i = \sum_m \eta_m e^{-(m-i)^2/L^2}$, where L is the correlation length and $\{\eta_m\}$ are uncorrelated random variables assigned from a normal distribution. This construction yields a spatially-correlated set of couplings obeying

$$\langle J_i J_j \rangle \sim \exp\left(-\frac{(i-j)^2}{L^2}\right). \tag{5}$$

To ensure a positive mean and a controlled width of the hopping distribution, while preserving the imposed correlations, we apply the nonlinear transformation $J_i \to 0.5 \times \tanh(J_i) + 1$. Physically, it is important that the coupling amplitudes retain a fixed sign (all positive, in this case). Allowing both positive and negative values would correspond to random π-phase shifts between neighboring sites, which would change the symmetry class of the system and mix the effects of amplitude disorder with those of sign (or phase) disorder. By enforcing a single sign for J_i, we isolate the role of amplitude fluctuations while keeping the overall topology and phase structure of the homogeneous array unchanged.

We assume the weak-coupling regime $\gamma \ll 1$, such that the atomic dynamics is influenced by the detunings $\omega_a - E_k$. In a fully ordered system, this regime entails Markovian dynamics in the center of the band, with the exponential decay of the atomic population $r(t) \equiv |f_e(t)|^2 = e^{-\gamma^2 t/J}$ [29]. This can be readily verified for $\gamma = 0.1J$, which we will fix throughout. The flatness of $G(E)$ in this case follows from the atom being strongly detuned from the band edges and, most importantly, from the field modes being described by Bloch wavefuncions. In contrast, if the environment is made up by localized wavefunctions, it may trigger resonant cavity-QED dynamics [22, 11]. These results reveal an interesting relationship between delocalization/localization and Markovianity/non-Markovianity [11], which we explore in the following section for the correlated off-diagonal disorder model introduced above.

3. Results

The time-evolved state $|\psi(t)\rangle = f_e(t)|e\rangle|\text{vac}\rangle + \sum_i f_i(t)|g\rangle|1_i\rangle$, with $|1_i\rangle = \hat{a}_i^\dagger|\text{vac}\rangle$ representing a photon occupying the local mode (cavity) i, is obtained by numerically integrating the Schrödinger equation using the fourth-order Runge-Kutta method. For computing larger array sizes N, we use a self-expanding chain technique. Instead of initializing the full array, we begin with a reduced segment centered around the emitter, covering about 100 cavities each side. During the time evolution, the wavefunction amplitude $|f_i(t)|$ at the edges of the self-expanding array is monitored, with the domain being dynamically expanded whenever non-negligible amplitudes are detected. Array sizes up to $N = 8000$ are considered, for maximum times $tJ \sim 2000$, ensuring no boundary effects. This adaptive approach ensures numerical precision while avoiding

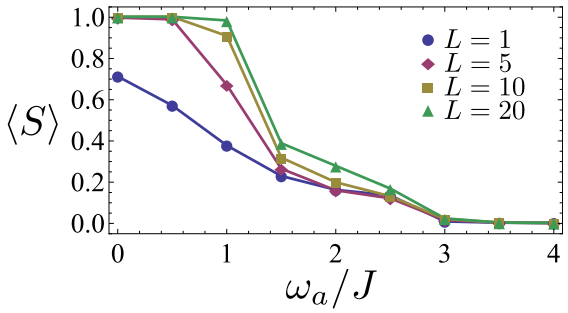

Figure 1: Time-averaged occupation probability of the array, $\langle S \rangle$, with $t_0 J \sim 1500$, as a function of the atomic frequency ω_a for different values of L. Each curve is averaged over 10^3 realizations of the disorder.

unnecessary computations, and is especially efficient for simulating photon dynamics in onedimensional lattices. We use a time step of $\Delta t \approx 0.008/J$, which provides reasonable accuracy and low computational cost, while keeping the norm of the wavefunction close to 1, with deviations on the order of 10^{-10}.

First, let us discuss the environment occupation probability, defined as $S(t) = \sum_i |f_i(t)|^2$, which characterizes the capability of the atom to release energy to the environment. We want to evaluate its long-time behavior by $\langle S \rangle = \frac{1}{N_T} \sum_{t_n > t_0} S(t_n)$, where the sum runs over times t_n beyond a transient threshold $t_0 = 1500/J$, and N_T is the number of points covered. This averaged quantity provides a robust indicator of the localization properties of the coupled-cavity array, with $\langle S \rangle \to 1$ indicating delocalization of the field modes in close resonance with the emitter's frequency ω_a.

Results are shown in Fig. 1 for distinct values of the correlation parameter L. We note that $\langle S \rangle$ responds more sharply to L up to $\omega_a = 1J$, suggesting that the correlation length favors states with large localization lengths around the center of the band, despite the array being disordered. Note that $\langle S \rangle \to 0$ does not necessarily imply the presence of localized field modes. Rather, it expresses that the atomic frequency reached a photonic bandgap and therefore cannot release its energy. Other outcomes of $\langle S \rangle$ indicate partial trapping of the atomic excitation, manifested due to an active atom-field energy exchange. We mention that atomic population trapping, accompanied by partial field localization, can occur even in the absence of disorder as a consequence of the formation of atom-photon bound states [28, 29].

To improve the analysis over the localization properties of the environment we compute eigenstate participation ratio defined as

$$\xi_k = \frac{1}{\sum_{i=1}^{N} |\langle 1_i | \alpha_k \rangle|^4}. \tag{6}$$

This quantity provides an estimate of the number of sites effectively occupied by the eigenstate, which ranges from 1 to N, corresponding fully localized and delocalized states, respectively. In Figs. 2(a–c) we present the quantity $\ln(\xi/N)$ as a function of $\ln(N)$ for different values of the correlation length L at selected frequencies E. For $L = 1$, all curves decay with N, indicating that ξ remains approximately constant as N increases. This is the expected behavior for localized states with

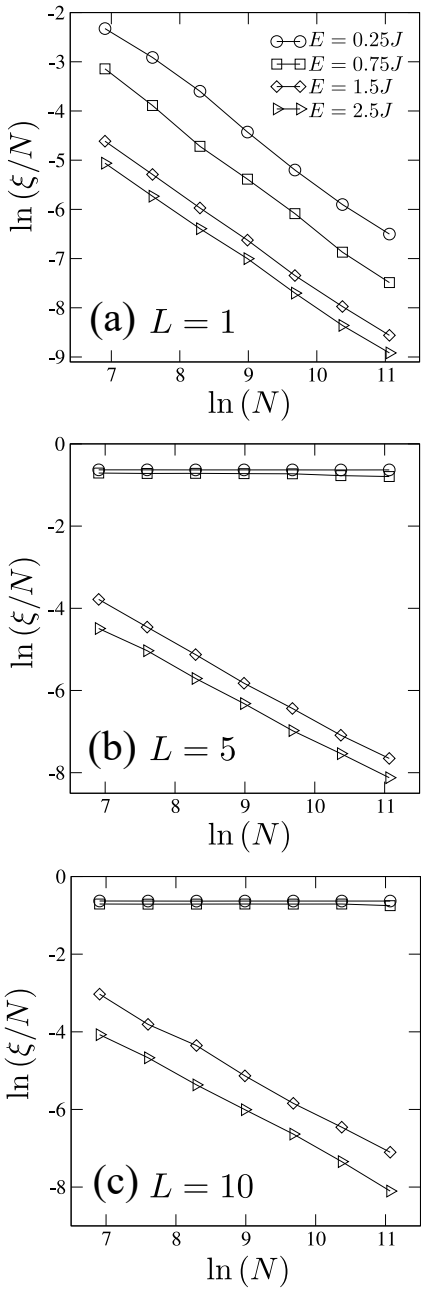

Figure 2: Participation ratio $\xi = \xi(E)$ evaluated at selected frequencies E of the bosonic environment. The plots show $\ln(\xi/N)$ versus $\ln(N)$ for correlation lengths (a) $L = 1$, (b) $L = 5$, and (c) $L = 10$. Results reveal a crossover from localized states ($L = 1$) to states with large localization lengths for $L > 1$ at low frequencies.

a finite localization length. In contrast, for $L > 1$ and $E < 1$, the rescaled participation ξ/N is approximately constant with increasing N, as evidenced by the slope ≈ 0. This behavior indicates that the corresponding eigenstates exhibit, within the range of system sizes N considered here, a localization length $\sim N$. For higher frequencies, ξ/N always decreases with N even for large correlation lengths L. Hence, the eigenstates remain localized. In summary, the eigenstates near the center of the frequency spectrum possess large localization lengths due to the presence of correlated disorder. An emitter weakly cou-

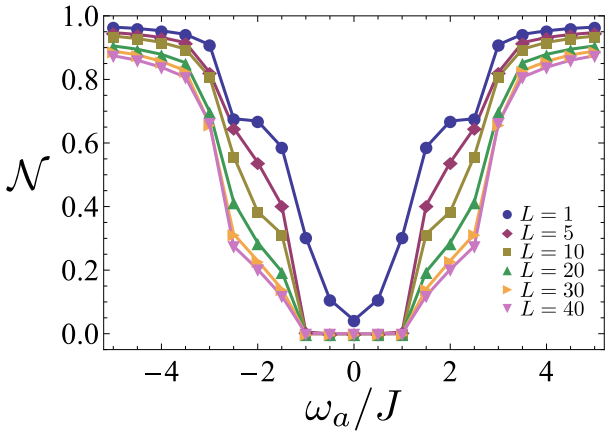

Figure 3: Non-Markovianity measure $\mathcal{N}$ as a function of the atomic frequency ω_a for many values of L. Each curve is averaged over an ensemble of 10^3 realizations of the disorder.

pled to the environment will thus hybridize mostly with those eigenstates whose frequencies are close to ω_a.

The next step is to compute the degree of non-Markovianity of the emission process across the range of frequencies. Numerous quantifiers for non-Markovianity exist in the literature [36, 37, 3, 38, 39], each suited to different physical scenarios. In our case, the system undergoes a pure amplitude damping process [11, 20], with well-defined limits: exponential decay corresponds to the Markovian regime, while full Rabi oscillations indicate extreme non-Markovianity. A suitable measure should capture the information backflow to the atom during the dynamics. We adopt a criterion based on the volume of accessible states [37], represented here by the squared return probability $r^2(t)$. For an amplitude damping channel it suffices to track the positive slopes of $\partial_t r(t)$ using the formula [11]:

$$\mathcal{N} = \frac{\displaystyle\int_{\partial_t r(t)>0} \frac{d}{dt}\left[r^2(t)\right] dt}{\left|\displaystyle\int_{\partial_t r(t)<0} \frac{d}{dt}\left[r^2(t)\right] dt\right|}, \tag{7}$$

where the denominator ensures that $\mathcal{N}$ ranges from 0 (Markovian dynamics) to 1 (maximum non-Markovianity).

Figure 3 illustrates the dependence of $\mathcal{N}$ against ω_a for different values of the correlation length L. For very short L ($L = 1$), $\mathcal{N}$ displays a dip at $\omega_a = 0$. This is related to the known anomaly in the localization length of the zero-energy modes in the presence of off-diagonal disorder [31]. As L increases, a clear Markovian regime spans from about $\omega = -J$ through J, with outcomes $\mathcal{N} \lesssim 10^{-8}$. Some degree of non-Markovianity is observed beyond that frequency range, with $\mathcal{N}$ increasing with ω_a – due to the influence of localized modes – eventually saturating with L. Note that the highest values of $\mathcal{N}$ occur for $|\omega_a| \gtrsim 3J$, that is, when the atomic frequency crosses the band edge.

To help with the interpretation of the results, in Fig. 4 we plot the spectral density function $G(E)$ of the coupled cavity array, for selected values of L, obtained by exact numerical diagonalization of $\hat{H}_{\rm env}$ [Eq. (4)]. For $L = 1$ and $L = 5$, only a *single* disorder sample is considered, so as to highlight the effect of the correlation length. The first shows an irregular, peaked profile across the band, but with weaker fluctuations near the band center, which explains the corresponding results for $\mathcal{N}$ [Fig. 3]. Now, remarkably, even with the slightest increase to $L = 5$, $G(E)$ becomes a smooth function over the region that corresponds to strong Markovianity. When the atom is weakly coupled to the environment, it effectively senses a flat $G(E)$. One example of $G(E)$ averaged over many disorder realizations is shown in the last panel of Fig. 4 for $L = 20$. Therein, we see that two well-defined peaks appear at $E \approx \pm J$. These peaks bridge the crossover between Markovian and non-Markovian emission regimes and surround environment modes possessing large localization lengths.

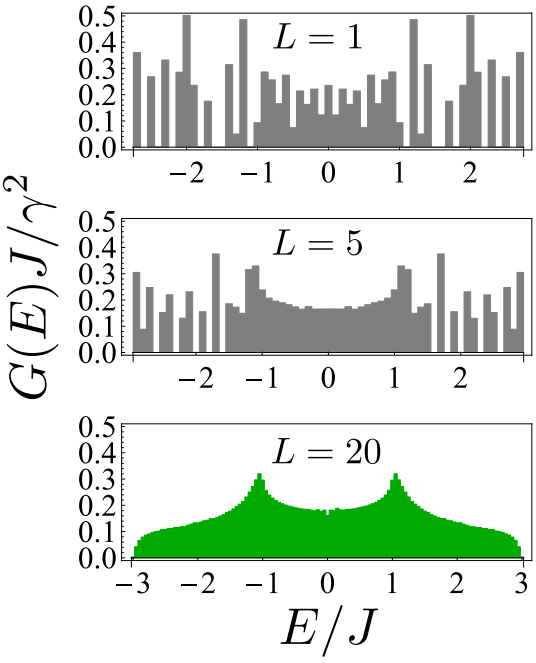

Figure 4: Spectral density $G(E) \equiv \sum_k |\gamma_k|^2 \delta(E - E_k)$ of the coupled-cavity array for selected values of L. Results are obtained via exact numerical diagonalization of the free-field Hamiltonian, Eq. (4), with $N = 1000$. A single (typical) disorder realization is employed for $L = 1, 5$, whereas an ensemble of size 10^3 is used for $L = 20$.

We remark that the type of correlated disorder considered in the present work, occurring in the hopping amplitudes, differs substantially from the more commonly studied case of correlated diagonal (on-site) disorder [20, 21]. Hopping disorder is characterized by a significantly larger localization length near the center of the band. This is why the obtained crossover between both emission regimes is so pronounced at definite resonant energies (see Fig. 3). We also examined (now shown) the same model but with Gaussian-correlated diagonal disorder. The behavior of the participation ratio ξ indicated much shorter localization lengths for the same set of parameters L and E. Appreciable Markovian dynamics would only appear in the immediate vicinity of $E = 0$ for very large L, which is a less interesting result.

Finally, let us comment on the relationship between non-Markovianity and the characteristic localization length of the resonant frequency by making an analogy with cavity-QED phenomena. Given the weak-coupling condition for γ, let us consider the approximation in which the atom strongly interacts with one of the modes, say α_ℓ, while the others effectively behave as a Markovian environment. A Lindblad master equation can then be written as (see details in Ref. [11]):

$$\dot{\rho} = -i[\hat{H}_\ell, \rho] + \Gamma\left(\hat{L}\rho\hat{L}^\dagger - \frac{1}{2}\left\{\hat{L}^\dagger\hat{L}, \rho\right\}\right), \tag{8}$$

where ρ is the reduced state of the atom plus mode ℓ. The dissipative modes act on the main partition via the jump operator $\hat{L} = \hat{\sigma}_-$ associated with the rate $\Gamma = \pi\sum_{k\neq\ell}|\gamma_k|^2\delta(E_k - \omega_a)$. Here, the atom coherently interacts with a dressed field mode, instead of a local cavity mode via [cf. Eq. (1)]

$$\hat{H}_\ell = \omega_a\hat{\sigma}_+\hat{\sigma}_- + E_\ell\hat{\alpha}_\ell^\dagger\hat{\alpha}_\ell + \gamma_\ell(\hat{\sigma}_+\hat{\alpha}_\ell + \text{h.c.}). \tag{9}$$

The master equation above accounts for a dissipative Jaynes-Cummings model. The most important factor in governing the damped Rabi dynamics is the ratio Γ/γ_ℓ. The larger it is, the closer the emission is to the Markovian regime.

To connect this effective model to the actual disordered coupled-cavity array, we need a criterion to select mode ℓ. Given the modes available for a given realization of the disorder and in the light of perturbation theory, mode ℓ can be chosen as the one that maximizes $|\gamma_\ell|/|E_k - \omega_a|$. Then, a relationship between cavity volume and localization length of the dominant mode can be established of the form $\gamma_\ell \propto \xi_\ell^{-1/2}$ [11]. Once this is set, the damping rate Γ can be calculated, which is proportional to the spectral density at ω_a excluding the contribution from mode ℓ.

We remark that the phenomenological model discussed above does not describe the actual time dynamics of our system. Rather, it encodes the main ingredients responsible for the memory effects seen in the atomic dynamics, namely the trade-off between Rabi oscillations and exponential decay. Another model in the same spirit was proposed in [20], based on a high-Q cavity under the influence of a Lorentzian spectral density. It is even possible to derive analytical expressions for $\mathcal{N}$ as a function of Γ/γ_ℓ. Here, we will limit ourselves to highlighting the general intuitive picture: as the participation ratio ξ of the modes in close resonance with ω_a increases, Γ becomes dominant, leading to a Markovian regime.

4. Conclusions

In this work, we studied the non-Markovianity of atomic emission into a coupled-cavity array featuring correlated hopping disorder, modeled by a Gaussian kernel with a characteristic correlation length L. This model provides a more realistic representation of physical systems where imperfections arise from correlated processes rather than completely random noise.

The Gaussian decay implies that cavities separated by a distance much larger than L become essentially uncorrelated, while parameter fluctuations involving nearby sites are effectively weaker. For large L this significantly affects the localization properties of wavefunctions, leading to large localization lengths around the band center. This, in turn, favors Markovian dynamics due to the weak atom-environment coupling. A crossover to non-Markovian behavior was observed at larger resonant frequencies ω_a, associated with the onset of localized modes.

We also computed the long-time occupation probability $\langle S\rangle$ across the coupled-cavity array after an initial transient. We obtained that $\langle S\rangle \to 1$ only in the Markovian regime due exponential nature of the emission. Otherwise, there will be significant trapping of the atomic population, which can be linked to the characteristic low participation ratio ξ of the modes involved as well as to the irregular shape of the spectral density function $G(E)$ featuring gaps [10]. We note, however, that in real systems atomic excitation may eventually escape through other dissipation channels in the long-time limit.

Disorder engineering in photonic lattices offers a promising venue to study and manipulate quantum dissipation in the context of cavity QED. Technological progress in field [25, 26, 27] motivates further studies along the direction of the results presented here. Extensions of this work may target on, e.g. higher-dimensional coupled-cavity systems [40], flat bands [41, 26], and other classes of correlated disorder [31].

Acknowledgements

This work was supported by FAPEAL, FACEPE, CAPES, and CNPq.

References

[1] A. G. Kofman, G. Kurizki, and B. Sherman. Spontaneous and induced atomic decay in photonic band structures. *Journal of Modern Optics*, 41(2):353–384, 1994.

[2] P Lambropoulos, Georgios M Nikolopoulos, Torben R Nielsen, and Søren Bay. Fundamental quantum optics in structured reservoirs. *Reports on Progress in Physics*, 63(4):455, apr 2000.

[3] Ángel Rivas, Susana F Huelga, and Martin B Plenio. Quantum non-markovianity: characterization, quantification and detection. *Reports on Progress in Physics*, 77(9):094001, aug 2014.

[4] S. Roshan Entezar. Entanglement of a two-level atom and its spontaneous emission near the edge of a photonic band gap. *Physics Letters A*, 373(38):3413–3418, 2009.

[5] Bi-Heng Liu, Li Li, Yun-Feng Huang, Chuan-Feng Li, Guang-Can Guo, Elsi-Mari Laine, Heinz-Peter Breuer, and Jyrki Piilo. Experimental control of the transition from markovian to non-markovian dynamics of open quantum systems. *Nature Physics*, 7(12):931–934, Dec 2011.

[6] Tony J. G. Apollaro, Carlo Di Franco, Francesco Plastina, and Mauro Paternostro. Memory-keeping effects and forgetfulness in the dynamics of a qubit coupled to a spin chain. *Phys. Rev. A*, 83:032103, Mar 2011.

[7] K. H. Madsen, S. Ates, T. Lund-Hansen, A. Löffler, S. Reitzenstein, A. Forchel, and P. Lodahl. Observation of non-markovian dynamics of a single quantum dot in a micropillar cavity. *Phys. Rev. Lett.*, 106:233601, Jun 2011.

[8] Tommaso Tufarelli, M. S. Kim, and Francesco Ciccarello. Non-markovianity of a quantum emitter in front of a mirror. *Phys. Rev. A*, 90:012113, Jul 2014.

[9] Zhong-Xiao Man, Nguyen Ba An, and Yun-Jie Xia. Non-markovian dynamics of a two-level system in the presence of hierarchical environments. *Opt. Express*, 23(5):5763–5776, Mar 2015.

[10] Heng-Na Xiong, Ping-Yuan Lo, Wei-Min Zhang, Da Hsuan Feng, and Franco Nori. Non-markovian complexity in the quantum-to-classical transition. *Scientific Reports*, 5(1):13353, Aug 2015.

[11] S. Lorenzo, F. Lombardo, F. Ciccarello, and G. M. Palma. Quantum non-markovianity induced by anderson localization. *Sci. Rep. 7*, 42729, 2017.

[12] Salvatore Lorenzo, Francesco Ciccarello, and G. Massimo Palma. Non-markovian dynamics from band edge effects and static disorder. *International Journal of Quantum Information*, 15(08):1740026, 2017.

[13] Steve Campbell, Francesco Ciccarello, G. Massimo Palma, and Bassano Vacchini. System-environment correlations and markovian embedding of quantum non-markovian dynamics. *Phys. Rev. A*, 98:012142, Jul 2018.

[14] Francesco Cosco and Sabrina Maniscalco. Memory effects in a quasiperiodic fermi lattice. *Phys. Rev. A*, 98:053608, Nov 2018.

[15] H. Z. Shen, Shuang Xu, H. T. Cui, and X. X. Yi. Non-markovian dynamics of a system of two-level atoms coupled to a structured environment. *Phys. Rev. A*, 99:032101, Mar 2019.

[16] Vasily E. Tarasov. Non-markovian dynamics of open quantum system with memory. *Annals of Physics*, 434:168667, 2021.

[17] Dominic Gribben, Aidan Strathearn, Gerald E. Fux, Peter Kirton, and Brendon W. Lovett. Using the Environment to Understand non-Markovian Open Quantum Systems. *Quantum*, 6:847, 2022.

[18] G. Mouloudakis and P. Lambropoulos. Coalescence of non-markovian dissipation, quantum zeno effect, and non-hermitian physics in a simple realistic quantum system. *Phys. Rev. A*, 106:053709, Nov 2022.

[19] Chandrashekhar Gaikwad, Daria Kowsari, Carson Brame, Xingrui Song, Haimeng Zhang, Martina Esposito, Arpit Ranadive, Giulio Cappelli, Nicolas Roch, Eli M. Levenson-Falk, and Kater W. Murch. Entanglement assisted probe of the non-markovian to markovian transition in open quantum system dynamics. *Phys. Rev. Lett.*, 132:200401, May 2024.

[20] Mariana O. Monteiro, Nadja K. Bernardes, Eugene M. Broni, Francisco A. B. F. de Moura, and Guilherme M. A. Almeida. Non-markovian to markovian decay in structured environments with correlated disorder. *Phys. Rev. A*, 111:022212, Feb 2025.

[21] Mariana O. Monteiro, Guilherme M.A. Almeida, and Francisco A.B.F. de Moura. Spontaneous emission in a coupled cavity array featuring random-dimer disorder. *Annals of Physics*, 477:170009, 2025.

[22] Luca Sapienza, Henri Thyrrestrup, Søren Stobbe, Pedro David Garcia, Stephan Smolka, and Peter Lodahl. Cavity quantum electrodynamics with anderson-localized modes. *Science*, 327(5971):1352–1355, 2010.

[23] Ulrich Hoeppe, Christian Wolff, Jens Küchenmeister, Jens Niegemann, Malte Drescher, Hartmut Benner, and Kurt Busch. Direct observation of non-markovian radiation dynamics in 3d bulk photonic crystals. *Phys. Rev. Lett.*, 108:043603, Jan 2012.

[24] Yanbing Liu and Andrew A. Houck. Quantum electrodynamics near a photonic bandgap. *Nature Physics*, 13(1):48–52, Jan 2017.

[25] Francesco Di Colandrea, Tareq Jaouni, John Grace, Dilip Paneru, Mirko Arienzo, Alessio D'Errico, and Ebrahim Karimi. Engineering qubit dynamics in open systems with photonic synthetic lattices. *Phys. Rev. Res.*, 7:023236, Jun 2025.

[26] Yu-Tong Wang, Qi-Hang Ye, Jun-Yong Yan, Yufei Qiao, Yu-Xin Liu, Yong-Zheng Ye, Chen Chen, Xiao-Tian Cheng, Chen-Hui Li, Zi-Jian Zhang, Cheng-Nian Huang, Yun Meng, Kai Zou, Wen-Kang Zhan, Chao Zhao, Xiaolong Hu, Clarence Augustine T. H. Tee, Wei E. I. Sha, Zhixiang Huang, Huiyun Liu, Chao-Yuan Jin, Lei Ying, and Feng Liu. Moiré cavity quantum electrodynamics. *Science Advances*, 11(21):eadv8115, 2025.

[27] Xiao-Bo Zhang, Su-Ming Weng, Hong Ai, Xin Qiao, Ju-Kui Xue, and Zheng-Ming Sheng. Photonic rabi oscillations in defective plasma photonic crystals. *Phys. Rev. Lett.*, 135:015101, Jul 2025.

[28] S. Longhi. Bound states in the continuum in a single-level fano-anderson model. *The European Physical Journal B*, 57(1):45–51, May 2007.

[29] F. Lombardo, F. Ciccarello, and G. M. Palma. Photon localization versus population trapping in a coupled-cavity array. *Phys. Rev. A*, 89, 2014.

[30] Francisco A. B. F. de Moura and Marcelo L. Lyra. Delocalization in the 1d anderson model with long-range correlated disorder. *Phys. Rev. Lett.*, 81:3735–3738, Oct 1998.

[31] F.M. Izrailev, A.A. Krokhin, and N.M. Makarov. Anomalous localization in low-dimensional systems with correlated disorder. *Physics Reports*, 512(3):125–254, 2012.

[32] I. A. Luchnikov, E. O. Kiktenko, M. A. Gavreev, H. Ouerdane, S. N. Filippov, and A. K. Fedorov. Probing non-markovian quantum dynamics with data-driven analysis: Beyond "black-box" machine-learning models. *Phys. Rev. Res.*, 4:043002, Oct 2022.

[33] J Barr, G Zicari, A Ferraro, and M Paternostro. Spectral density classification for environment spectroscopy. *Machine Learning: Science and Technology*, 5(1):015043, mar 2024.

[34] A. L. C. Pereira, C. H. Lewenkopf, and E. R. Mucciolo. Correlated random hopping disorder in graphene at high magnetic fields: Landau level broadening and localization properties. *Phys. Rev. B*, 84:165406, Oct 2011.

[35] H.P. Breuer and F. Petruccione. *The Theory of Open Quantum Systems*. Clarendon, 2002.

[36] Ángel Rivas, Susana F. Huelga, and Martin B. Plenio. Entanglement and non-markovianity of quantum evolutions. *Physical Review Letters*, 105(5):050403, 2010.

[37] Salvatore Lorenzo, Francesco Plastina, and Mauro Paternostro. Geometrical characterization of non-markovianity. *Phys. Rev. A*, 88:020102, Aug 2013.

[38] Heinz-Peter Breuer, Elsi-Mari Laine, Jyrki Piilo, and Bassano Vacchini. Colloquium: Non-markovian dynamics in open quantum systems. *Rev. Mod. Phys.*, 88:021002, Apr 2016.

[39] Thiago Melo D. Azevedo, Cristhiano Duarte, and Nadja K. Bernardes. Distillation of quantum non-markovianity. *Physics Letters A*, 512:129582, 2024.

[40] Guilherme M. A. Almeida and Andre M. C. Souza. Quantum transport with coupled cavities on an apollonian network. *Phys. Rev. A*, 87:033804, Mar 2013.

[41] Enrico Di Benedetto, Alejandro Gonzalez-Tudela, and Francesco Ciccarello. Dipole-dipole interactions mediated by a photonic flat band. *Quantum*, 9:1671, March 2025.